A computational study of carbene ligand stabilization of biomimetic models of the rotated Hred state of [FeFe]-hydrogenase

Article (Accepted Version)

A Computational Study of Carbene Ligand Stabilization of Biomimetic Models of the Rotated H_{red} State of [FeFe]-Hydrogenase

Bitupon Borthakur[a], Alfredo Vargas[b] and Ashwini K. Phukan*[a]

[a] Mr. Bitupon Borthakur, Prof. Ashwini K. Phukan
E-Mail: ashwini@tezu.ernet.in
Homepage URL: http://www.tezu.ernet.in/dcs/personal_profile_akp.html
Department of Chemical Sciences, Tezpur University, Napaam 784028, Assam, India

[b] Dr. Alfredo Vargas
Department of Chemistry, School of Life Sciences, University of Sussex, Brighton, BN1 9QJ, Sussex, United Kingdom

Abstract: Stabilization of *fully* rotated conformation at one of the iron center has been achieved for the reduced Fe(I)Fe(I) state in chelated cyclic alkyl amino carbene (CAAC) substituted biomimetic hydrogenase model complex. This study indicates that the spatial orientation of the chelated NHCs at one of the iron center plays a major role in determining the geometry at the other iron center. We also made an attempt at explaining the electronic origin behind the favorability of rotated vs unrotated structure in asymmetrically substituted chelated vs monodentate NHC complexes.

Introduction:

The non-renewable and hazardous nature of fossil fuels has prompted the scientists to look for alternative sustainable fuels which can fulfill the increasing demand of energy. Dihydrogen (H_2) is one of the possible solutions for this because it is a promising source of energy and can be considered as a "zero-emission" fuel. Therefore, many researchers devoted their studies towards effective production of dihydrogen via proton reduction.[1] Nature can do this very efficiently using an enzyme called hydrogenase which can be classified into three main categories as [NiFe], [FeFe] and [Fe] – hydrogenase based on the metal ion composition of their active sites.[2,3] [FeFe] – hydrogenase catalyze the reversible activation of dihydrogen (equation 1) involving two key intermediates (H_{ox} and H_{red}, Scheme 1).[3c-d,f]

$$H_2 \rightleftharpoons H^- + H^+ \rightleftharpoons 2H^+ + 2e^- \qquad (1)$$

The active site of [FeFe] – H_2ase contains a bimetallic sub cluster [Fe_2S_2] and a [Fe_4S_4] cubane (all together known as H – cluster) linked through a cysteinyl sulphur group.[4] The Fe atoms are referred to as proximal (Fe_p) and distal (Fe_d) with respect to the [Fe_4S_4] cubane and

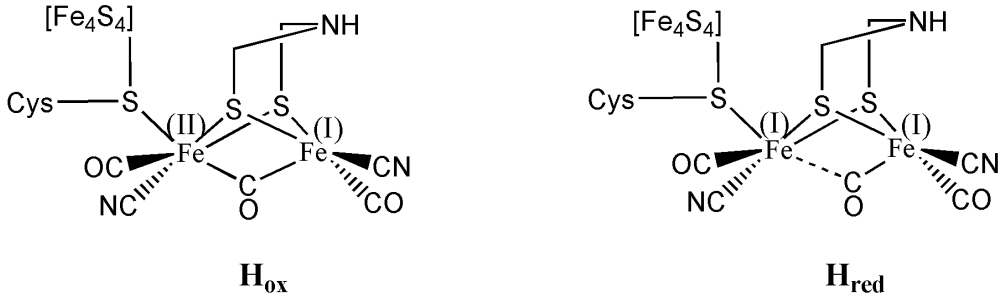

H_{ox} **H_{red}**

Scheme 1: Schematic structures for the active site of [FeFe] – hydrogenase, left: oxidized or mixed valence state (H_{ox}), right: reduced state (H_{red}).

each metal atom contains one CN^- and one CO group. In addition, one CO group bridges the two Fe atoms in the oxidized state (i.e. H_{ox})[4,5] which transforms to semi-bridging position on one electron reduction (i.e. in H_{red} state).[3e-f,6] The bimetallic site also contains a cofactor which bridges the two metal centers known as dithiolate cofactor ($-SCH_2XCH_2S-$). There has been a lot of debate regarding the composition of this cofactor particularly about the nature of the bridgehead atom.[7] However, recent studies provide strong evidence in support of a nitrogen atom i.e., the bridging cofactor is actually an azadithiolate group.[8]

Since the structural characterization of the active site of [FeFe] – H_2ase, several experimental and theoretical studies were carried out to mimic the active site of this enzyme with model complexes.[1b-d,f,9,10,11] While some of them deal with better understanding of the structural features,[1b-c,9] others focus on the mechanistic study of the catalytic pathways.[1f,10] One of the important structural features of the H_{ox} and H_{red} state of the native enzyme is the presence of an inverted square pyramidal or fully rotated geometry at Fe_d. The only structural difference between the oxidized (Fe^{II}-Fe^{I}) and reduced (Fe^{I}-Fe^{I}) state is that the carbonyl group between the metal centers is in a semi-bridging position in the H_{red} state, unlike in a completely bridging position in H_{ox} state. The vacant site at Fe_d is the probable site for coordination of H^+/H_2 during reversible dihydrogen production.[12] In 2013, the research groups of Schollhammer[9c] and

Rauchfuss[9d] independently reported two model complexes featuring a fully rotated conformation at one of the Fe atom in the reduced Fe^{I}-Fe^{I} state (**A** and **B**, Scheme 2). They reported that the simultaneous presence of three structural features, *viz*, (1) desymmetrization of the two Fe centers, (2) presence of bulky substituent at the dithiolate linkage and most importantly (3) presence of intramolecular agostic interaction between the rotated Fe atom and the dithiolate substituent are necessary to obtain a rotated geometry in the Fe^{I}-Fe^{I} state. Previous studies by Hsieh et al. also suggest that steric hindrance from the bridgehead substituents impose significant distortions in biomimetic models for the reduced Fe^{I}-Fe^{I} state (**C** and **D**, Scheme 2).[13] In addition, very recently Weigand *et al.* isolated a sterically stabilized [FeFe]-hydrogenase model complex which exhibits a semi-rotated conformation in Fe^{I}-Fe^{I} state (**E**, Scheme 2).[14]

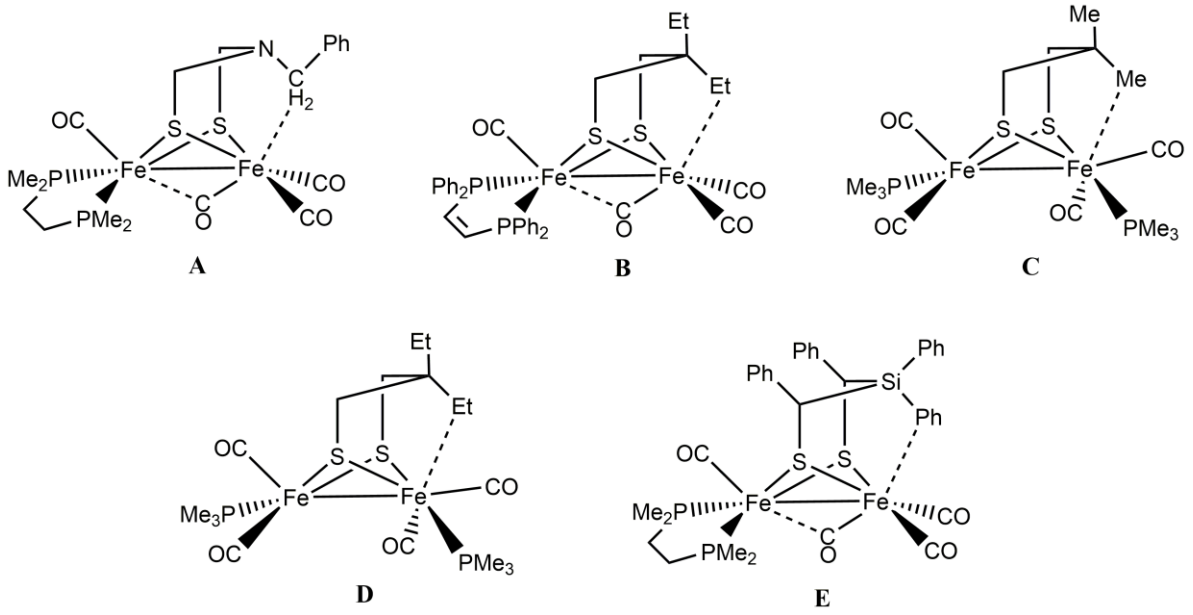

Scheme 2: Crystallographically characterized structures of the model complexes with inverted square pyramidal geometry at one of the Fe centers in the Fe^{I}-Fe^{I} state.

There were reports of *N*-heterocyclic carbenes (NHC) being used as cyanide mimic in the active site models of [FeFe] – H_2ase and few model complexes containing NHCs both in the reduced and oxidized states have been reported.[1b-d,9b,15] Interestingly, Darensbourg et al. discussed the rotated structure of the model complex $\{(\mu\text{-pdt})[Fe(CO)_2PMe_3][Fe(CO)_2IMes]\}^+$ in the mixed valence state which resembles the H_{ox} state of the native enzyme.[15] However, to the best of our knowledge, till date there is no model complex for the [FeFe] – H_2ase active site bearing NHCs as ligand with a *rotated* structure at one of the Fe center in the reduced Fe^I-Fe^I state. It may be noted that in all these studies, only Arduengo type carbenes were considered while a range of NHCs are known with varying degree of electronic properties.[16] Accordingly, we have investigated the structural features of model complexes with a variety of structurally and electronically different heterocyclic carbenes. In this report, we summarize the results obtained from an exploratory study about the possibility of obtaining a rotated structure in the Fe^I-Fe^I state. The model complexes studied were unsymmetrically substituted by both monodentate and chelated NHCs and the bridging cofactor between the two Fe centers is an azadithiolate linkage.

Computational Details: All the structures were fully optimized in the gas phase without any geometric constraint using BP86 functional[17] incorporated within the Gaussian 03 suit of program.[18a] Even though various studies have reported the validity of this functional in reproducing the structural features of hydrogenase model complexes,[9c-d,10e,h,19] we carried out calculations on some representative molecules using hybrid PBE0[20] as well as meta-GGA M06[21] exchange-correlation functional. Interestingly, the key geometrical parameters (e.g., Fe_p-Fe_d bond lengths) computed at BP86 level are in better agreement with the experimental values for similar carbene substituted model complexes compared to those computed using PBE0 and

M06 functional (Table S1, Supporting Information). We have used Def2-TZVP basis set for Fe and Def2-SVP for all other atoms.[22] Calculations using Def2-TZVP basis set for all the atoms with more than 1600 basis functions are much beyond the scope of our available computational resources. However, we indeed performed calculations on few representative molecules using Def2-TZVP basis set for all the atoms and found only marginal differences on the key geometrical parameters as well as on the energy differences between the possible isomers (Tables S1 and S2, Supporting Information). Also, solvent (acetonitrile) and dispersion effects were evaluated for these molecules using polarizable continuum model (PCM)[23] and D3 version of Grimme's dispersion correction coupled with D3 damping function using the keyword "Empirical Dispersion = GD3" as implemented in Gaussian 09 suit of programs.[18b] The nature of the optimized geometries are characterized by calculating their vibrational frequencies at the same level of theory and all of them were found to be minima with real frequencies. It should be noted that we have also considered the high spin triplet state for some representative molecules which were found to be in higher energy by 18-28 kcal mol^{-1} (Table S3, Supporting Information). Further, broken symmetry calculations were performed on few representative molecules employing the wave functions generated from fragments of the compounds under consideration. Interestingly, it has been found that the broken symmetry singlet states lie at higher energy compared to the respective closed shell singlet states (Table S4, Supporting Information) which validates the use of spin-restricted calculations for the present work.

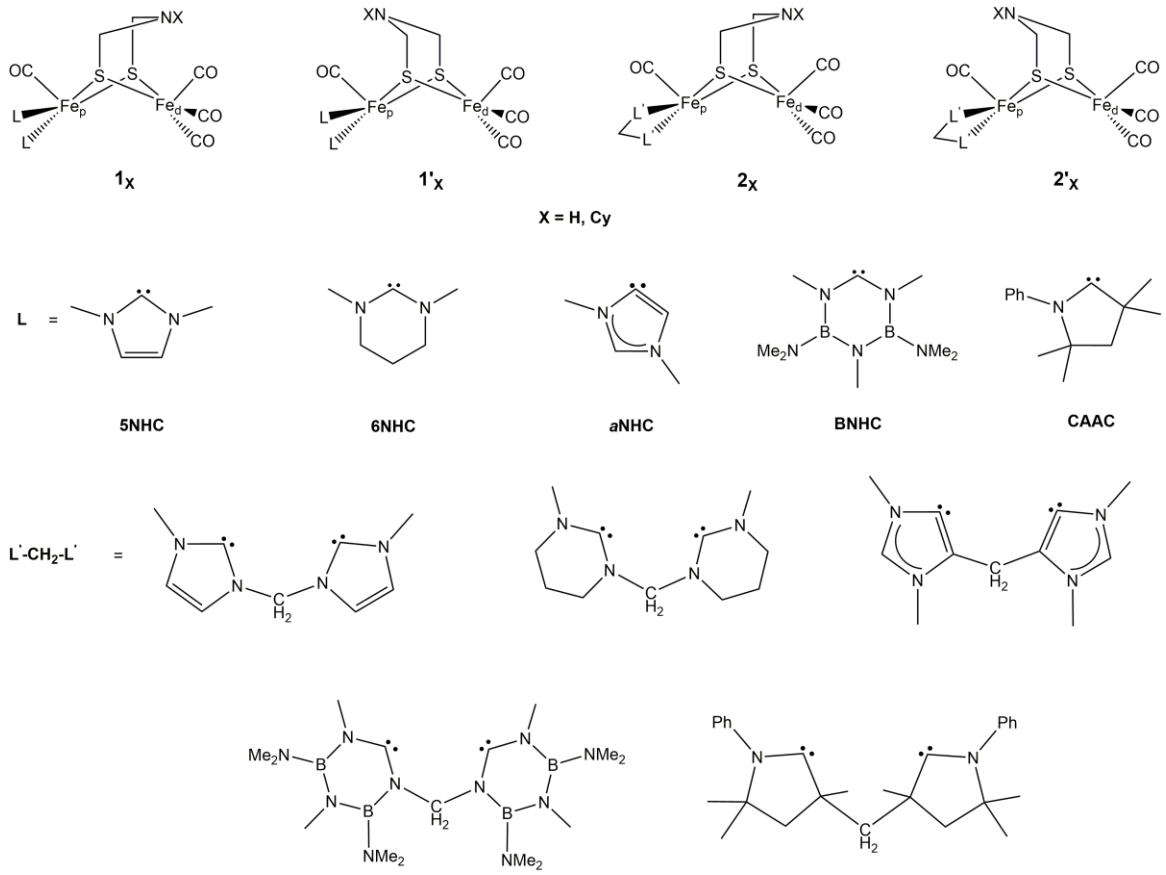

Scheme 3: Schematic representation of the molecules considered in the present study (X= H/Cyclohexyl)

Before discussing the results, it is necessary to give a description about the nomenclature of the model complexes investigated in this study. The models for the bimetallic active site can be represented by the general formulae (μ-$(SCH_2)_2NX)[Fe(CO)_3][Fe(CO)L_2]$ and (μ-$(SCH_2)_2NX)[Fe(CO)_3][Fe(CO)(L'\text{-}CH_2\text{-}L')]$ for the monodentate and chelated complexes respectively where X = H/Cyclohexyl and L/L′ = NHCs. A schematic representation of all the molecules considered in this work is given in Scheme 3. We divided the molecules into two main categories – **1** (with monodentate NHCs) and **2** (with chelated NHCs). The isomers obtained by

flipping the azadithiolate linkage are indicated as **1′**and **2′.** The subscript H and Cy is used for X=H and cyclohexyl respectively (e.g. $\mathbf{1_H}$ and $\mathbf{1_{Cy}}$).

Results and Discussion:

Unsymmetrical substitution of the diiron center for the Fe(I)Fe(I) state is carried out using both monodentate and chelated NHCs. In all of these complexes, we have considered only the basal/basal isomer with respect to NHC coordination at Fe as X-ray diffraction study confirms that the bis-carbene ligand is in a basal/basal environment in similar experimentally known complexes.[1c] Further, the recent synthesis of diiron compounds modeling the H_{red} state has the electron donor phosphorus arms at the basal positions.[9c,d] The carbene substituted Fe center is referred as proximal (Fe_p) whereas the other one as distal (Fe_d) (Scheme 3).

Model Complexes with Normal Five-membered NHCs (5NHC): As mentioned above, we have considered both monodentate and chelated 5NHCs as the substituents for the proximal iron center (Fe_p). However, we did not get rotated structures for monodentate 5NHCs as substituents at Fe_p even though the $Fe_d(CO)_3$ unit is distorted to some extent (C_{CO}-Fe_p-Fe_d-C_{CO} dihedral angle is 16.2° and 7.7° for $\mathbf{1_H}$**-5NHC** and $\mathbf{1'_H}$**-5NHC** respectively, where C_{CO} stands for carbonyl carbon). The distortion is somewhat greater for complexes with bulky substituent (i.e. cyclohexyl) in the azadithiolate group. In case of the chelated complexes, initially we have installed the 5NHC ligands at Fe_p in a similar orientation (Scheme 4(a)) as that in the experimentally known model complex [(μ-pdt)[Fe(*Che*-5NHC)$(CO)_4$][1c] (*Che* = chelated) having an unrotated geometry. As expected, optimization of all the chelated complexes ($\mathbf{2_X}$**-5NHC** and $\mathbf{2'_X}$**-5NHC**) lead to unrotated structures.

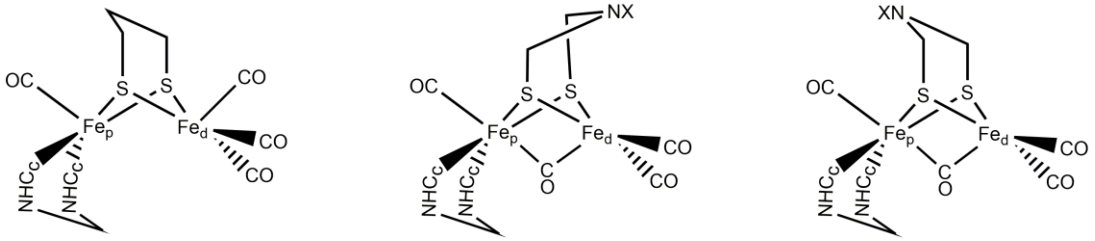

Scheme 4: Schematic representations of the orientation of the chelated 5NHC ligands in (a) **[(*μ*-pdt)[Fe(*Che*-5NHC)(CO)$_4$]**, and rotated starting geometries for (b) **2$_X$-5NHC** and (c) **2'$_X$-5NHC**, where X= H/Cy. The carbenic carbon atoms are indicated by Cc.

Further, optimizations starting from rotated geometries in which the chelated NHC rings are positioned below the Fe_p–Fe_d bond vector (Schemes 4(b) and 4(c)), lead to unrotated structures for both the flipped complexes (**2'$_X$-5NHC**) as well as for the parent complex having hydrogen as the azadithiolate substituent (**2$_H$-5NHC**). Interestingly, for the parent complex having cyclohexyl group at the azadithiolate bridgehead (**2$_{Cy}$-5NHC**) the rotated structure is preserved during optimization. However, it should be noted that the rotated isomer obtained for **2$_{Cy}$-5NHC** is found to be unstable compared to the respective un-rotated ones (Table S5, Supporting Information). All these observations indicate that the unrotated geometries will be the most favoured ones as far as orientation of the *Che*-5NHC below the Fe_p–Fe_d bond is concerned (Figure S1(a), Supporting Information). The instability of the rotated conformers may be attributed to the presence of steric hindrance below the Fe-Fe bond which sterically prevent the movement of one of the basal CO unit at the distal iron center to a bridging position between the iron centers. Therefore, we envisage that it may be possible to get the rotated conformation for all these complexes by considering a different orientation of the chelated 5NHCs around Fe_p.

Accordingly, we have optimized all the chelated complexes starting from an unrotated geometry where the NHC rings are moved away from the proximal iron center (Scheme 5(a)) thus making room for transfer of a CO group at Fe_d to occupy a bridging position between Fe_p and Fe_d centres. Interestingly, complete rotation of the $Fe_d(CO)_3$ unit is observed with this particular

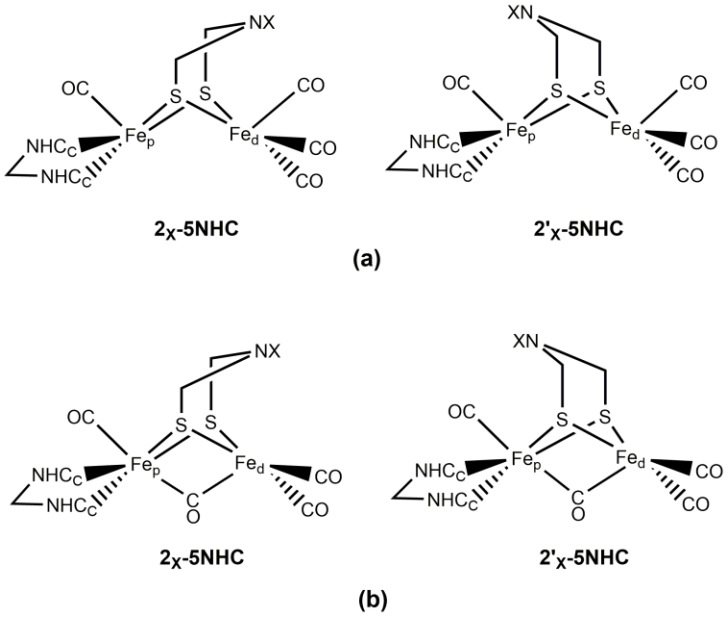

Scheme 5: Schematic representations of the orientation of the chelated 5NHC ligands in (a) unrotated and (b) rotated starting geometries for **2_X-5NHC** and **$2'_X$-5NHC**, where X= H/Cy. The carbenic carbon atoms are indicated by Cc.

orientation of chelated 5NHCs around Fe_p thereby resulting in an inverted square pyramidal geometry at Fe_d with a semi-bridging carbonyl group between the two iron centers (Figure S2, Supporting Information) implying that the orientation of the chelated NHC ligands at Fe_p plays a crucial role in determining the geometry at Fe_d. Further, optimizations were also performed starting from rotated geometries where the chelated 5NHCs orients away from the proximal iron center as shown in Scheme 5(b) and Figure S1(b). As expected, all these complexes preserve

their rotated form in the optimized states as well. This indicates that irrespective of the nature of the starting geometry (*i.e.*, rotated or unrotated) one can get the rotated structure for all these model complexes if and only if the *Che*-NHCs orients away from the proximal iron center. Coordination of the chelated NHCs forms a six-membered metallacycle at Fe_p (Fe_p-C_c-N-C-N-C_c ring, C_c stands for carbene carbon) which adopts a boat like conformation (Figure S3, Supporting Information). The calculated values of Addison τ parameter[24] for the rotated structures (Table S6, Supporting Information) are also in accordance with a perfectly inverted square-pyramidal, *i.e.*, fully-rotated geometry at Fe_d. In addition, the C_{CO}-Fe_p-Fe_d-C_{CO} dihedral angle is also found to be significantly large (107.3°). It is found that the chelated complexes with rotated geometries have substantially shorter Fe_p-Fe_d bond lengths (2.595-2.605Å) compared to those with monodentate ones (*i.e.*, **1_X-5NHC** and **$1'_X$-5NHC**, 2.715-2.741Å). The reduced Fe_p-Fe_d bond lengths for the rotated complexes may be attributed to the presence of semi-bridging carbonyl group which binds both the iron centers. An MO analysis for **1_H-5NHC** and **2_H-5NHC** (Figure 1) shows that in **1_H-5NHC**, the MO representing the Fe_p-Fe_d bonding interaction is HOMO-1 (-4.1 eV) while in **2_H-5NHC**, both HOMO-6 (-5.4 eV) and HOMO-8 (-5.6 eV) contribute to the

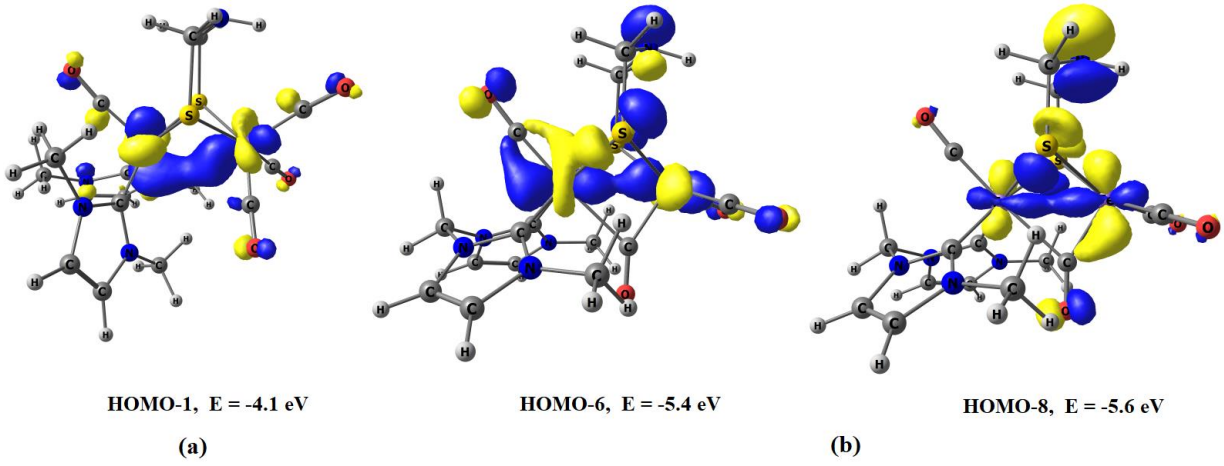

Figure 1: Molecular orbitals representing the Fe_p-Fe_d bonding interaction in (a) **1_H-5NHC** and (b) **2_H-5NHC**.

.aforementioned interaction. It should be noted that HOMO-6 of **2_H-5NHC** has dominant contribution (~55%) from both the iron centers comprising major contributions from $d_{X^2-Y^2}$ (12.8%) orbital of Fe_d and d_{XZ} (13.6%) and $d_{X^2-Y^2}$ (13.8%) orbitals of Fe_p respectively. Similarly, HOMO-8 has ~39% contribution from both the iron centers having contributions from d_{XZ} (11%) orbital of Fe_p and d_{XZ} (11%) and d_{Z^2} (11.7%) orbitals of Fe_d respectively.

It should be noted that the rotated structure of the flipped isomer **$2'_H$-5NHC** is found to lie in higher energy (by 2.6 kcal mol^{-1}) than that of the parent one (**2_H-5NHC**) thereby indicating that the non-bonded interaction (between Fe_d·····HN) gives an additional stabilization to the rotated geometry which is in accordance with previous studies.[9c-d,14] Inclusion of solvent and dispersion in the computational model found to have marginal effect on the energy difference (ΔE = 2.8 kcal mol^{-1}) between the parent and flipped isomer. The ΔE value increases to 3.2 kcal mol^{-1} at the PBE0/Def2-TZVP level of theory and further increases to 3.9 kcal mol^{-1} on being computed using the meta-GGA M06 functional. Similar is the case for complexes with bulky azadithiolate substituent where the un-flipped isomer (**2_{Cy}-5NHC**) is found to be 4.8 kcal mol^{-1} more stable than the flipped isomer (**$2'_{Cy}$-5NHC**). Interestingly, the calculated ν_{CO} values for **2_{Cy}-5NHC** are very close to the theoretically assigned values for the recently reported biomimetic complex having a rotated geometry.[9d]

However, the rotated isomers obtained for **2_X-5NHC** and **$2'_X$-5NHC** complexes considering the NHC orientations away from the Fe_p center (Scheme 5) are found to be unstable than the unrotated ones (by 5.6 - 11.4 kcal mol^{-1}, Table S7, Supporting information) which explains why [(μ-pdt)[Fe(*Che*-5NHC)$(CO)_4$] gets crystalized in an unrotated form despite the presence of chelated 5NHCs. It should be noted that the rotated structure is observed (although higher in energy) only with chelated 5NHCs and accordingly, we have considered only the

chelated versions of the remaining four different types of NHCs (Scheme 3) as substituents at the proximal iron center.

Model Complexes with Normal Six-membered NHCs (6NHC), Abnormal NHCs (*a*NHC) and Boron Substituted NHCs (BNHC): Optimizations were carried out using the chelated versions of these three types of NHCs (Scheme 3) by considering all the four different starting geometries as shown in Schemes 4 and 5 and the results are found to be akin to the case with chelated 5NHCs. Even though we obtained rotated structures for **2_{Cy}-*a*NHC** considering *Che*-NHC orientations as shown in Scheme 4(b), the same is found to be unstable compared to the respective unrotated one (Table S5, Supporting Information). Interestingly, here also, complete rotation of the $Fe_d(CO)_3$ unit is observed when the chelated NHCs orients away from the proximal iron center as shown in Scheme 5(a). However, unfortunately all these three types of NHCs also fail to stabilize the rotated conformer as compared to the unrotated ones (Table S7, Supporting Information). It may be noted that the energy difference between the rotated and unrotated isomers of **2_{Cy}-*a*NHC** is comparatively lower (4.2 kcal mol^{-1}) as compared to all other complexes and the computed average ν_{CO} value for **$2'_{Cy}$-*a*NHC** (1921 cm^{-1}) is very close to the average ν_{CO} value obtained for the reduced form of the enzyme *Desulfovibrio desulfuricans* (average 1925 cm^{-1}).[5b]

Model Complexes with Cyclic Alkyl Amino Carbene (CAAC): Recent advances in carbene chemistry shows that cyclic(alkyl)(amino)carbene (CAAC) possesses better ligand properties than classical NHCs in terms of both electron donation and acceptance ability.[15a-c,25] Therefore, we have considered CAAC as one of the possible substituent at the proximal iron site and the

chelation of the two CAAC ligands were carried out through the sp^3 hybridized carbon atoms (Scheme 3). Optimizations of all the chelated CAAC substituted complexes starting from a geometry where the orientation of the chelated CAAC ligands is similar to that in the experimentally isolated one (Scheme 4(a)) lead to unrotated structures with all terminal CO groups at Fe_d. However, we obtained a rotated structure for **2_{Cy}-CAAC** starting from a rotated starting geometry as shown in Scheme 4(b). Unfortunately, the rotated form lies at higher energy compared to the respective unrotated one (Table S5, Supporting Information) with similar *Che*-CAAC orientation. Further, incorporation of chelated CAAC groups at Fe_p similar to that shown in Scheme 5(a) leads to rotation of the $Fe_d(CO)_3$ unit and results in a perfectly inverted square pyramidal geometry which is confirmed by the calculated values of Addison τ parameter (Table S4, Supporting Information). Similarly, starting from a rotated structure as shown in Scheme 5(b) also lead to the same rotated geometry as obtained starting from an unrotated one. However, as compared to the previous complexes with all the variants of NHCs, the energy difference between the rotated and unrotated isomers for the complexes **2_H-CAAC** and **2_{Cy}-CAAC** are minimal. In fact, the rotated isomer of **2_{Cy}-CAAC** is found to be slightly more stable (by 0.45 kcal mol^{-1}) than the unrotated one which increases to 5.4 kcal mol^{-1} as a result of inclusion of dispersion in the computational model. To confirm it further, we have performed additional calculations using the dispersion corrected WB97XD and the meta-GGA M06 functional and both these functional too indicate the higher stability (by 4.0 kcal mol^{-1}) of the rotated isomer of **2_{Cy}-CAAC**. Further, the computed $Fe_d\cdots H_{Cy}$ bond distance in the rotated isomer of **2_{Cy}-CAAC** (2.781 Å) is in close agreement with experimentally reported model complex for the H_{red} state with a rotated geometry (Fe·····HC = 2.750 Å).[9c] All these observations for the rotated isomer of **2_{Cy}-CAAC** is in accordance with previous experimental studies for the fully rotated structure in

asymmetrically substituted [FeFe]-hydrogenase model complex with a bulky substituent at the dithiolate bridgehead. The preference of CAAC for a rotated conformer may be attributed to both electronic and steric factors. First of all, CAAC is a strong donor as compared to conventional NHCs which will significantly increase the electron density at the proximal iron center thereby favouring rotation of the $Fe_d(CO)_3$ unit (*vide infra*). Further, CAAC possesses bulky phenyl groups at position α to the carbene center and accordingly, it will favour the rotated conformer where the carbenes orients away from Fe_p thereby minimizing the steric hindrance between the substituents of the two iron centers. It is also worthwhile to mention that the energy difference between the rotated and the more stable unrotated isomers of **2_H-CAAC** is only 1.8 kcal mol^{-1} thereby indicating that depending on the experimental conditions, one isomer may be preferred over the other. Interestingly, the average ν_{CO} value for **2_H-CAAC** (1925 cm^{-1}) is in excellent agreement with that obtained for the reduced form of the enzyme *Desulfovibrio desulfuricans*.[5b] Further, **2_{Cy}-CAAC** also possesses average ν_{CO} values (1918 cm^{-1}) which is very close to that observed for enzyme active site.

To Rotate or not to Rotate? The Role of Chelation: It should be noted that we observe complete rotation of the $Fe_d(CO)_3$ unit only for the complexes with chelated NHC ligands (even though the rotated structure is higher in energy than the unrotated one for most of the cases) but not with the monodentate ones. Accordingly, to unravel the role of chelation toward obtaining the rotated geometry, we have performed an in depth molecular orbital analysis for **1_H-CAAC** and **2_H-CAAC** and the results are discussed below.

The rotation of $Fe_d(CO)_3$ unit in the chelated complexes is a consequence of significant increase in electron density at the proximal iron center. In case of the monodentate complexes, there is a minor difference in the interaction of one of the CAAC ligands with the proximal iron

center compared to the other which may be attributed to the difference in spatial orientation of both the CAACs. However, replacement of one methyl group on each CAAC by the methylene group in the chelated complexes reduces the repulsion between them thereby resulting in stronger overlap between the carbene lone pair orbitals and vacant d-orbital of the iron center which is further corroborated by the calculated shorter Fe_p-C_C bond lengths for the chelated complex (1.970/1.970 Å) compared to those with monodentate ones (1.980/1.990 Å). A closer look at Figure 2 shows that in **1_H-CAAC**, the lone pair orbital of one of the CAAC ligands weakly overlap with the vacant metal d-orbital while both the donor sites interact equally in **2_H-CAAC** thereby forming two equal Fe_p-C_c bonds. In addition, the chelate bite angle ($\angle C_C$-Fe_p-C_C) is also found to be smaller in **2_H-CAAC** (93.4°) compared to that in **1_H-CAAC** (96.4°). Further, the increase in electron density at the proximal iron center upon chelation of the CAACs (*i.e.,* in **2_H-CAAC**) is also evident from an increase in the values of natural charge (-0.284) and natural valence population (8.222) at Fe_p compared to those in **1_H-CAAC** (-0.117 and 8.064 respectively). The electron rich proximal iron center undergoes electronic relaxation by transferring some of the excess electron density to the π*-orbital of one of the basal CO group at Fe_d thereby bringing this CO group to a semi-bridging position (Figure 3). The stepwise changes in Fe_p-Fe_d bonding interaction as well as the formation of new Fe_p-CO_{bridg} bond during inversion of the $Fe_d(CO)_3$ unit for **2_H-CAAC** is shown in Figure 4.

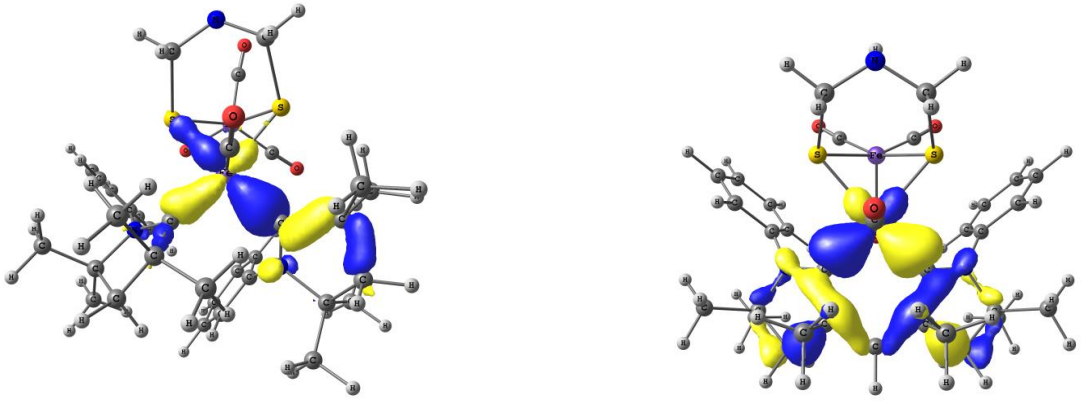

(a) (b)

Figure 2: Molecular orbital representing the overlap between the lone pairs of CAAC and metal d-orbitals in (a) **1_H-CAAC** and (b) **2_H-CAAC**.

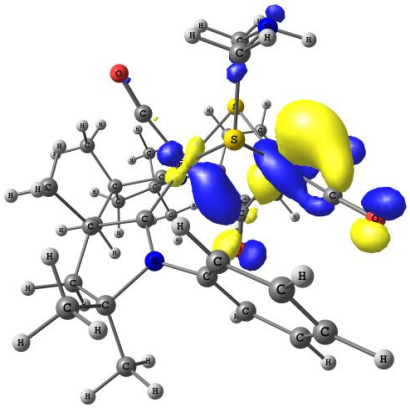

Figure 3: Molecular orbital showing the interaction between the proximal iron center (Fe_p) and bridging carbonyl group in **2_H-CAAC**.

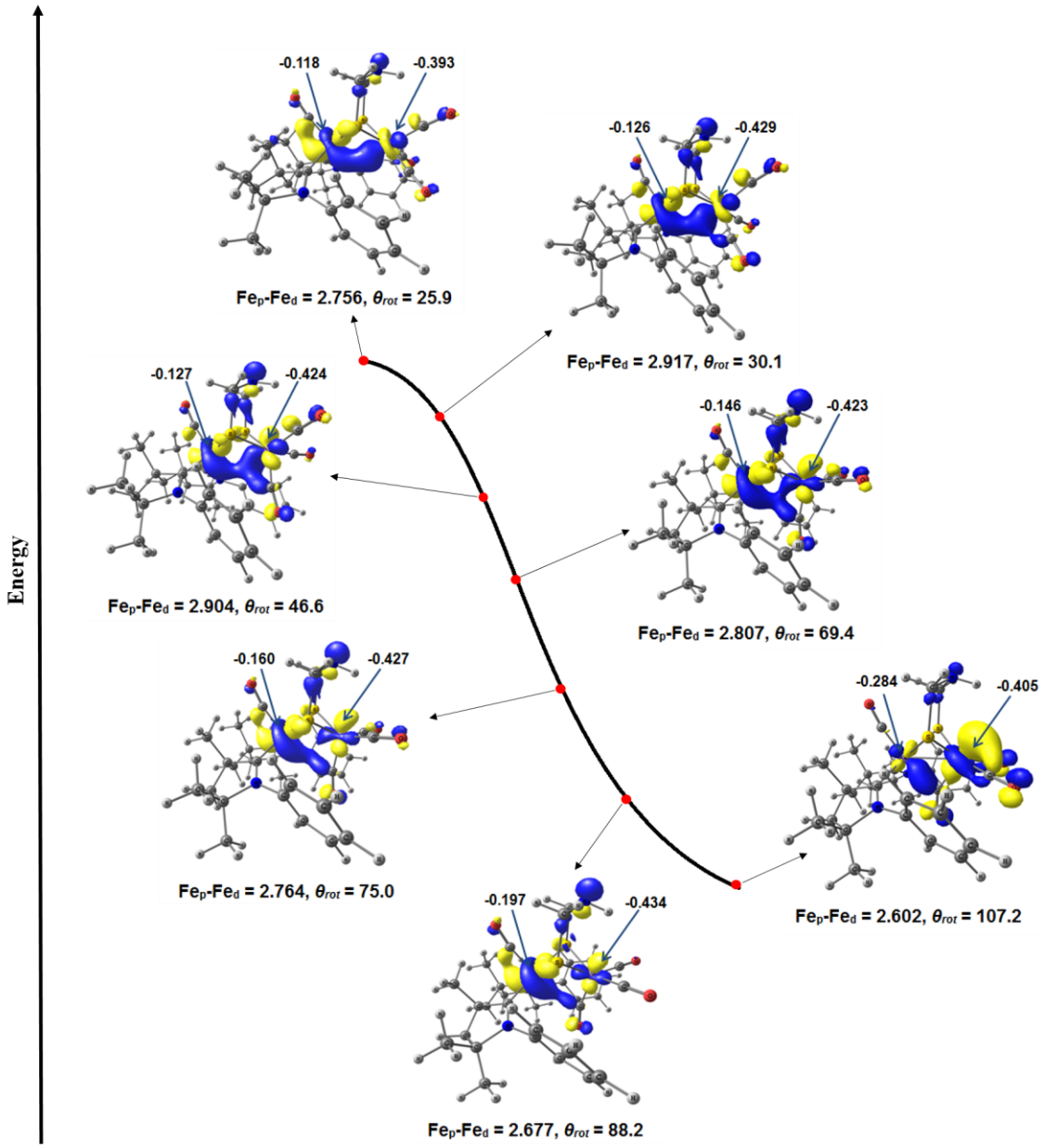

Figure 4: Molecular orbitals showing the stepwise changes in Fe_p-Fe_d bonding interaction as well as formation of new Fe_p-CO_{bridg} bond during rotation of $Fe_d(CO)_3$ unit in **2_H-CAAC**. The values represented by the arrows are natural charges at Fe_p (left) and Fe_d (right). θ_{rot} ($\angle C_{CO}$-Fe_p-Fe_d-C_{CO}) represents the dihedral angle reflecting rotation at $Fe_d(CO)_3$ unit (C_{CO} represents carbon atom of the carbonyl group). The values of Fe_p-Fe_d bond lengths and θ_{rot} are given in Å and degrees respectively.

Conclusions: This theoretical study reveals that chelation of the carbenes at the proximal iron center may lead to a fully rotated structure for the [FeFe]-hydrogenase model complexes. The rotation is facilitated by increase in electron density at the proximal iron center due to stronger overlap of the chelated carbene lone pairs with the vacant metal d-orbital. However, such orbital interaction is bit weaker for the complexes with monodentate carbenes. The spatial orientation of the chelated carbenes at the proximal iron center plays a major role in determining the geometry at the distal iron center. Our study highlights the fact that as far as rotation at one of the iron center is concerned, except CAAC, all other carbenes considered in this study failed to achieve this feat and hence they may not be ideal candidates for experimental studies. Interestingly, the CAAC anchored complexes such as **2_H-CAAC** and **2_{Cy}-CAAC** are found to be suitable candidate towards obtaining a rotated structure and invite experimental verification. In addition, the higher stability of the rotated isomer of **2_{Cy}-CAAC** as compared to the unrotated one is in accordance with the previous experimental observation of fully rotated structure in asymmetrically substituted complex with a bulky substituent at the dithiolate bridgehead. In view of the paucity of biomimetic model complexes with a rotated structure for the H_{red} state of [FeFe]-hydrogenase, we hope that our study will inspire experimental chemists towards designing of model systems with a rotated structure.

Supporting Information:

Cartesian coordinates of all the molecules along with their total energies including zero point vibrational correction and table containing different calculated parameters.

Acknowledgements:

A.K.P. thanks Council of Scientific and Industrial Research (CSIR), New Delhi for providing financial assistance in the form of a project (project no. 01(2912)/17/EMR-II). B. B. thanks CSIR for Senior Research Fellowship. The computational facilities provided by CDAC Pune at Tezpur University are also gratefully acknowledged. A.V. thanks the University of Sussex for financial support. We thank an anonymous reviewer for very insightful comments that helped us in improving the quality of the manuscript.

Keywords:

[FeFe]-Hydrogenase, H_{red} State, Rotated Conformation, CAAC, Chelation

References:

1. a) J. L. Nehring, D. M. Heinekey, *Inorg. Chem.* **2003**, *42*, 4288-4292; b) J. Capon, S. E. Hassnaoui, F. Gloaguen, P. Schollhammer, J. Talarmin, *Organometallics* **2005**, *24*, 2020-2022; c) D. Morvan, J. Capon, F. Gloaguen, A. L. Goff, M. Marchivie, F. Michaud, P. Schollhammer, J. Talarmin, J. J. Yaouanc, *Organometallics* **2007**, *26*, 2042-2052; d) D. Morvan, J. Capon, F. Gloaguen, F. Y. Pétillon, P. Schollhammer, J. Talarmin, J. J. Yaouanc, F. Michaud, N. Kervarec, *J. Organometal. Chem.* **2009**, *694*, 2801-2807; e) M. K. Harb, U. Apfel, T. Sakamoto, M. El-Khateeb, W. Weigand, *Eur. J. Inorg. Chem.* **2011**, 986-993; f) M. E. Carroll, B. E. Barton, T. B. Rauchfuss, P. J. Carroll, *J. Am. Chem. Soc.* **2012**, *134*, 18843-18852; g) M. Bourrez, R. Steinmetz, F. Gloaguen, *Inorg. Chem.* **2014**, *53*, 10667-10673; h) F. Gloaguen, *Inorg. Chem.* **2016**, *55*, 390-398.
2. a) M. W. W. Adams, *Biochim. Biophys. Acta (BBA)-Bioenerg.* **1990**, *1020*, 115-145; b) S. P. J. Albract, *Biochim. Biophys. Acta (BBA)-Bioenerg.* **1994**, *1188*, 167-204; c) E. Garcin, X. Vernede, E. C. Hatchikian, A. Volbeda, M. Frey, J. C. Fontecilla-Camps,

Structure **1999**, *7*, 557-566; d) M. Korbas, S. Vogt, W. Meyer-Klaucke, E. Bill, E. J. Lyon, R. K. Thauer, S. Shima, *J. Biol. Chem.* **2006**, *281*, 30804-30813.

3. a) P. E. M. Siegbahn, J. W. Tye, M. B. Hall, *Chem. Rev.* **2007**, *107*, 4414-4435; b) W. Lubitz, E. Reijerse, M. v. Gastel, *Chem. Rev.* **2007**, *107*, 4331-4365; c) J. C. Fontecilla-Camps, A. Volbeda, C. Cavazza, Y. Nicolet, *Chem. Rev.* **2007**, *107*, 4273-4303; d) C. Tard, C. J. Pickett, *Chem. Rev.* **2009**, *109*, 2245-2274; e) W. Lubitz, H. Ogata, O. Rüdiger, E. Reijerse, *Chem. Rev.* **2014**, *114*, 4081-4148; f) T. R. Simmons, G. Berggren, M. Bacchi, M. Fontecave, V. Artero, *Coord. Chem. Rev.* **2014**, *270-271*, 127-150.
4. a) J. W. Peters, W. N. Lanzilotta, B. J. Lemon, L. C. Seefeldt, *Science* **1998**, *282*, 1853-1858; b) Y. Nicolet, C. Piras, P. Legrand, C. E. Hatchikian, J. C. Fontecilla-Camps, *Structure* **1999**, *7*, 13-23.
5. a) Z. J. Chen, B. J. Lemon, S. Huang, D. J. Swartz, J. W. Peters, K. A. Bagley, *Biochemistry* **2002**, *41*, 2036-2043; b) W. Roseboom, A. L. de Lacey, V. M. Fernandez, E. C. Hatchikian, S. P. J. Albracht, *J. Biol. Inorg. Chem.* **2006**, *11*, 102-118.
6. Y. Nicolet, A. L. de Lacey, X. Vernede, V. M. Fernandez, E. C. Hatchikian, J. C. Fontecilla-Camps, *J. Am. Chem. Soc.* **2001**, *123*, 1596-1601.
7. a) S. Foerster, M. v. Gastel, M. Brecht, W. Lubitz, *J. Biol. Inorg. Chem.* **2005**, *10*, 51-62; b) M. Brecht, M. v. Gastel, T. Buhrke, B. Friedrich, W. Lubitz, *J. Am. Chem. Soc.* **2003**, *125*, 13075-13083; c) A. S. Pandey, T. V. Harris, L. J. Giles, J. W. Peters, R. K. Szilagyi, *J. Am. Chem. Soc.* **2008**, *130*, 4533-4540.
8. a) D. Schilter, T. B. Rauchfuss, *Angew. Chem. Int. Ed.* **2013**, *52*, 13518-13520; b) A. Adamska-Venkatesh, S. Roy, J. F. Siebel, T. R. Simmons, M. Fontecave, V. Artero, E. Reijerse, W. Lubitz, *J. Am. Chem. Soc.* **2015**, *137*, 12744-12747; c) G. Berggren, A.

Adamska, C. Lambertz, T. R. Simmons, J. Esselborn, M. Atta, S. Gambarelli, J. M. Mouesca, E. Reijerse, W. Lubitz, T. Happe, *Nature* **2013**, *499*, 66-69; d) J. Esselborn, C. Lambertz, A. Adamska-Venkatesh, T. Simmons, G. Berggren, J. Noth, J. Siebel, A. Hemschemeier, V. Artero, E. Reijerse, M. Fontecave, *Nature Chemical Biology* **2013**, *9*, 607-609.

9. a) M. Bruschi, P. Fantucci, L. D. Gioia, *Inorg. Chem.* **2004**, *43*, 3733-3741; b) J. W. Tye, J. Lee, H. Wang, R. Mejia-Rodriguez, J. H. Reibenspies, M. B. Hall, M. Y. Darensbourg, *Inorg. Chem.* **2005**, *44*, 5550-5552; c) S. Munery, J. Capon, L. D. Gioia, C. Elleouet, C. Greco, F. Y. Pétillon, P. Schollhammer, J. Talarmin, G. Zampella, *Chem. Eur. J.* **2013**, *19*, 15458-15461; d) W. Wang, T. B. Rauchfuss, C. E. Moore, A. L. Rheingold, L. D. Gioia, G. Zampella, *Chem. Eur. J.* **2013**, *19*, 15476-15479.
10. a) M. T. Olsen, B. E. Barton, T. B. Rauchfuss, *Inorg. Chem.* **2009**, *48*, 7507-7509; b) C. Liu, J. N. T. Peck, J. A. Wright, C. J. Pickett, M. B. Hall, *Eur. J. Inorg. Chem.* **2011**, *43*, 1080-1093; c) J. M. Camara, T. B. Rauchfuss, *Nature Chemistry* **2012**, *4*, 26-30; d) Y. Wang, M. S. G. Ahlquist, *Dalton Trans.* **2013**, *42*, 7816-7822; e) C. Greco, *Inorg. Chem.* **2013**, *52*, 1901-1908; f) M. Bourrez, R. Steinmetz, F. Gloaguen, *Inorg. Chem.* **2014**, *53*, 10667-10673; g) W. Wang, T. B. Rauchfuss, L. Zhu, G. Zampella, *J. Am. Chem. Soc.* **2014**, *136*, 5773-5782; h) M. T. Huynh, W. Wang, T. B. Rauchfuss, S. Hammes-Schiffer, *Inorg. Chem.* **2014**, *53*, 10301-10311.
11. a) M. Y. Darensbourg, E. J. Lyon, X. Zhao, I. P. Georgakaki, *PNAS*, **2003**, *100*, 3683-3688. b) M. L. Singleton, R. M. Jenkins, C. L. Klemashevich, M. Y. Darensbourg, *Comptes Rendus Chimie*, **2008**, *11*, 861-874. c) M. L. Singleton, N. Bhuvanesh, J. H. Reibenspies, M. Y. Darensbourg, *Angew. Chem. Int. Ed.* **2008**, *47*, 9492-9495.

12. A. L. D. Lacey, V. M. Fernéndez, M. Rousset, R. Cammack, *Chem. Rev.* **2007**, *107*, 4304-4330.

13. C. H. Hsieh, O. F. Erdem, S. D. Harman, M. L. Singleton, E. Reijerse, W. Lubitz, C. V. Popescu, J. H. Reibenspies, S. M. Brothers, M. B. Hall, M. Y. Darensbourg. *J. Am. Chem. Soc.* **2012**, *134*, 13089-13102.

14. R. Goy, L. Bertini, C. Elleouet, H. Görls, G. Zampella, J. Talarmin, L. De Gioia, P. Schollhammer, U. P. Apfel, W. Weigand, *Dalton Trans.* **2015**, *44*, 1690-1699.

15. a) T. Liu, M. Y. Darensbourg, *J. Am. Chem. Soc.* **2007**, 129, 7008-7009; b) C. M. Thomas, T. Liu, M. B. Hall, M. Y. Darensbourg, *Inorg. Chem.* **2008**, *47*, 7009-7024.

16. a) V. Lavallo, Y. Canac, C. Präsang, B. Donnadieu, G. Bertrand, *Angew. Chem. Int. Ed.* **2005**, *44*, 5705-5709; b) V. Lavallo, Y. Canac, A. DeHope, B. Donnadieu, G. Bertrand, *Angew. Chem. Int. Ed.* **2005**, *44*, 7236-7239; c) M. Soleilhavoup, G. Bertrand, *Acc. Chem. Res.* **2015**, *48*, 256-266; d) C. Präsang, B. Donnadieu, G. Bertrand, *J. Am. Chem. Soc.* **2005**, 127, 10182-10183; e) K. E. Krahulic, G. D. Enright, M. Parvez, R. Roesler, *J. Am. Chem. Soc.* **2005**, *127*, 4142-4143; f) M. Iglesias, D. J. Beetstra, J. C. Knight, L. Ooi, A. Stasch, S. Coles, L. Male, M. B. Hursthouse, K. J. Cavel, A. Dervisi, I. A. Fallis, *Organometallics* **2008**, *27*, 3279-3289.

17. a) A. D. Becke, *Phys. Rev. A* **1988**, *38*, 3098-3100; b) J. P. Perdew, *Phys. Rev. B* **1986**, *33*, 8822.

18. a) M. J. Frisch, G. W. Trucks, H. B. Schlegel, G. E. Scuseria, M. A. Robb, J. R. Cheeseman, J. A., Jr. Montgomery, T. Vreven, K. N. Kudin, J. C. Burant, J. M. Millam, S. S. Iyengar, J. Tomasi, V. Barone, B. Mennucci, M. Cossi, G. Scalmani, N. Rega, G. A. Petersson, H. Nakatsuji, M. Hada, M. Ehara, K. Toyota, R. Fukuda, J. Hasegawa, M.

Ishida, T. Nakajima, Y. Honda, O. Kitao, H. Nakai, M. Klene, X. Li, J. E. Knox, H. P. Hratchian, J. B. Cross, V. Bakken, C. Adamo, J. Jaramillo, R. Gomperts, R. E. Stratmann, O. Yazyev, A. J. Austin, R. Cammi, C. Pomelli, J. W. Ochterski, P. Y. Ayala, K. Morokuma, G. A. Voth, P. J. Salvador, J. Dannenberg, V. G. Zakrzewski, S. Dapprich, A. D. Daniels, M. C. Strain, O. Farkas, D. K. Malick, A. D. Rabuck, K. Raghavachari, J. B. Foresman, J. V. Ortiz, Q. Cui, A. G. Baboul, S. Clifford, J. Cioslowski, B. B. Stefanov, G. Liu, A. Liashenko, P. Piskorz, I. Komaromi, R. L. Martin, D. J. Fox, T. Keith, M. A. Al- Laham, C. Y. Peng, A. Nanayakkara, M. Challacombe, P. M. W. Gill, B. Johnson, W. Chen, M. W. Wong, C. Gonzalez, J. A. Pople, *Gaussian 03*, revision D.02; Gaussian, Inc.: Pittsburgh, PA, **2003**; b) M. J. Frisch, G. W. Trucks, H. B. Schlegel, G. E. Scuseria, M. A. Robb, J. R. Cheeseman, G. Scalmani, V. Barone, B. Mennucci, G. A. Petersson, H. Nakatsuji, M. Caricato, X. Li, H. P. Hratchian, A. F. Izmaylov, J. Bloino, G. Zheng, J. L. Sonnenberg, M. Hada, M. Ehara, K. Toyota, R. Fukuda, J. Hasegawa, M. Ishida, T. Nakajima, Y. Honda, O. Kitao, H. Nakai, T. Vreven, J. A. Montgomery, Jr., J. E. Peralta, F. Ogliaro, M. Bearpark, J. J. Heyd, E. Brothers, K. N. Kudin, V. N. Staroverov, R. Kobayashi, J. Normand, K. Raghavachari, A. Rendell, J. C. Burant, S. S. Iyengar, J. Tomasi, M. Cossi, N. Rega, J. M. Millam, M. Klene, J. E. Knox, J. B. Cross, V. Bakken, C. Adamo, J. Jaramillo, R. Gomperts, R. E. Stratmann, O. Yazyev, A. J. Austin, R. Cammi, C. Pomelli, J. W. Ochterski, R. L. Martin, K. Morokuma, V. G. Zakrzewski, G. A. Voth, P. Salvador, J. J. Dannenberg, S. Dapprich, A. D. Daniels, Ö. Farkas, J. B. Foresman, J. V. Ortiz, J. Cioslowski, D. J. Fox, Gaussian 09, Revision D.01, Gaussian, Inc., Wallingford CT, **2009**.

19. a) C. Greco, L. D. Gioia, *Inorg. Chem.* **2011**, *50*, 6987-6995; b) G. Filippi, F. Arrigoni, L. Bertini, L. D. Gioia, G. Zampella, *Inorg. Chem.* **2015**, *54*, 9529-9542.

20. a) J. P. Perdew, K. Burke, M. Ernzerhof, *Phys. Rev. Lett.* **1996**, *77*, 3865; b) J. P. Perdew, K. Burke, M. Ernzerhof, *J. Chem. Phys.* **1996**, *105*, 9982-9985; c) M. Ernzerhof, G. E. Scuseria, *J. Chem. Phys.* **1999**, *110*, 5029-5036.

21. Y. Zhao, D. G. Truhlar, *Theor. Chem. Acc.* **2008**, *120*, 215-241.

22. a) F. Weigend, *Phys. Chem. Chem. Phys.* **2006**, *8*, 1057-1065; b) F. Weigend, R. Alhrichs, *Phys. Chem. Chem. Phys.* **2005**, *7*, 3297-3305.

23. a) M. Cossi, G. Scalmani, N. Rega, V. Barone, *J. Chem. Phys.* **2002**, *117*, 43-54; b) J. Tomasi, M. Persico, *Chem. Rev.* **1994**, *94*, 2027-2094.

24. A. W. Addison, T. N. Rao, J. Reedijk, J. v. Rijn, G. C. Verschoor, *J. Chem. Soc. Dalton Trans.* **1984**, 1349-1356.

25. a) M. Melaimi, R. Jazzar, M. Soleilhavoup, G Bertrand, *Angew. Chem. Int. Ed.* **2017**, *56*, 10046-10068 and references therein; b) S. Roy, K. C. Mondal, H. W. Roesky, *Acc. Chem. Res*. **2016**, *49*, 357-369.

Graphical Abstract

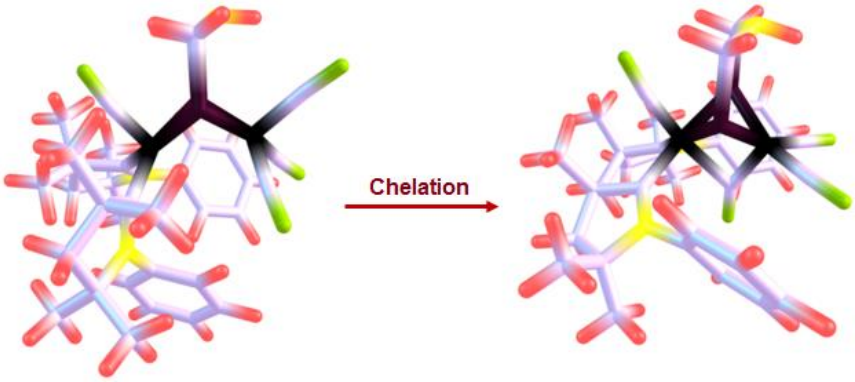

Computational analysis reveals the possible stabilization of fully rotated geometry in asymmetrically substituted chelated CAAC model complexes for the H_{red} state of [FeFe]-hydrogenase.